PERGAMON

International Journal of Heat and Mass Transfer 45 (2002) 5191–5200

International Journal of HEAT and MASS TRANSFER

www.elsevier.com/locate/ijhmt

Evolution of convection pattern during the solidification process of a binary mixture: effect of initial solutal concentration

P.V. Skudarnov, C.X. Lin, M.H. Wang, N. Pradeep, M.A. Ebadian *

Hemispheric Center for Environmental Technology, Center for Engineering and Applied Sciences, Florida International University, 10555 West Flagler Street, EAS-2100, Miami, FL 33174, USA

Received 21 June 2001; received in revised form 7 June 2002

Abstract

The evolution of convection pattern during the solidification of a binary mixture of ammonium chloride and water in a rectangular chamber was investigated experimentally. The solidification was carried out under a constant coolant temperature of −20 °C along the vertical walls of the test chamber. The convection patterns were obtained with the particle image velocimetry technique. The temperature distribution in the chamber was measured with a thermocouple rake. The initial concentrations of ammonium chloride ranged from 10 to 22 wt.%.

The present paper presents detailed description of the transient evolution of the convection pattern during the solidification process.

Keywords: Solidification; Binary mixture; Convection; Rectangular chamber

1. Introduction

Solidification has found many important applications in industry, such as metal castings and crystal growth. The flow in the liquid phase near the vicinity of a growing solid has profound consequences for the structure and composition of the solidified layer [1,2]. The evolution of the convection pattern is primarily responsible for macrosegregation within the cast metal and for defect distribution in the case of crystal growth. Hence, a better understanding of the evolution of the convection pattern during solidification for binary and multi-component mixtures is important in certain industrial solidification processes. In a binary mixture, the density of the liquid varies with both temperature and concentration. Thus, natural convection can be caused by thermally and solutally induced density gradients, often called double-diffusive convection [3].

In order to understand double-diffusive flow during the solidification process, it is necessary to ascertain the temperature and concentration distribution as well as the convective flow pattern in the liquid. Beckermann et al. [4–6] and Christenson et al. [7,8] have performed various studies on the multiple-point measurements of temperature and concentration fields during the solidification of aqueous solutions. Nishimura et al. [9,10] performed temperature and flow visualization using liquid crystals during solidification of an aqueous solution of ammonium chloride in a rectangular chamber with lateral cooling of one vertical wall. Temperature and concentration at several positions were simultaneously measured by thermocouples and by sample extraction with micro-syringes. Multiple-point measurements of concentrations show a step change in the vertical direction, and the temperature visualizations reveal S-shaped isotherms, which indicate the existence of time-dependent horizontally stacked roll-cells separated by diffusive interfaces. The concentration in each convective cell remains nearly constant although the thickness of each cell increases as the solidification process continues.

* Corresponding author. Tel.: +1-305-348-4238/3585; fax: +1-305-348-1852/4176.

E-mail address: ebadian@hcet.fiu.edu (M.A. Ebadian).

0017-9310/02/$ - see front matter
PII: S0017-9310(02)00224-7

Nomenclature

A_d	depth of the chamber	C_e	eutectic concentration of a binary solution
A_h	height of the chamber	t	solidification time
A_s	height of the solution within the chamber	T	fluid temperature
A_w	width of the chamber	T_e	eutectic temperature of a binary solution
C_w	weight concentration of NH_4Cl in water		

Han and Kuehn [11] studied double-diffusive natural convection experimentally and numerically in a rectangular chamber with an aspect ratio reaching up to 4. The layered multicell flow structure in the chamber for both assisting and opposing flow was visualized and also simulated by the numerical method. Dong and Ebadian [12] investigated double-diffusive convection in a trapezoidal chamber with the lateral thermal and solutal gradients imposed on the sidewalls of the chamber. They also numerically simulated double-diffusive convection in a V-shaped sump [13]. For both geometries, the multilayered flow structure was depicted in both assisting and opposing flow under certain conditions of buoyancy force ratio. In the high or low buoyancy force ratio, a unicell flow was predicted. The variation of the mean Nusselt number and Sherwood number with the buoyancy force ratio had the same tendency between the rectangular and the trapezoidal chambers. However, the numerical prediction of the convection flow pattern needs to be validated experimentally.

Despite the considerable effects of the double-diffusive phenomenon on solidification, very little attention has been paid to measuring the convection during solidification quantitatively. Reliable quantitative data of the convection pattern during the solidification/crystal growth process are scarce. The rapid progress in computational capability, on both the numerical side and the hardware side, is intriguing for the numerical prediction of the solidification process. However, the application of numerical prediction to industry needs a strict assessment of the validation of numerical algorithms and models. It becomes an urgent need as the benchmark for the solidification process.

The introduction of the particle image velocimetry (PIV) technique has made it possible to identify the convection pattern quantitatively during the solidification process. Wang et al. [14,15] reported the first investigation that employed a PIV system to study double-diffusive velocity profiles during the solidification process. They observed that a transient vortex type of convective flow occurred in the liquid region during the latter stage of the solidification of NH_4Cl–H_2O solution in a rectangular chamber. The vortex changed the original flow direction (downward along the vertical solidified surfaces in the liquid region of the test chamber) to the opposite direction. Experimental observation also showed that the vortex flow only occurs at a very low concentration of NH_4Cl (<2 wt.%) and that the cooling rate does not influence the formation of the vortex flow.

Pradeep et al. [16] compared the convection pattern during solidification of a binary mixture of NH_4Cl–H_2O under different thermal boundary conditions. Basically, the comparison was made for two rectangular chambers. For the first chamber, three surfaces (i.e., two side surfaces and one bottom surface) were cooled. For the second chamber, however, only two side surfaces were cooled. The experiments were conducted for a binary mixture at very low concentrations, and the cooling temperature ranged from -15 to -30 °C. The study suggested that the formation of vortex flow in the bottom corners was due to the cooling condition imposed on the bottom of the chamber. Therefore, the thermal boundary condition has a significant influence on the convection pattern during solidification.

The present study is a continuation of previous investigations on the measurement of convection pattern during the solidification process using the PIV technique. The purpose of this investigation was to reveal the effect of initial solutal concentration of aqueous ammonium chloride on the evolution of the convection pattern during the solidification process. The fluid velocities as well as the temperature profiles were measured for initial solutal concentrations of aqueous ammonium chloride ranging from 10 to 22 wt.%. With the understanding that the non-uniformity of the macrosegregation in cast metal or crystal growth is closely related to the convective cell structure formed in the solidification process, the present paper presents detailed description of the transient evolution of the convection pattern during the solidification process. The quantitative data from the present study may serve as a benchmark data set for the development of numerical simulation techniques for the prediction of the solidification process.

2. Experimental system

2.1. Test setup

The schematic diagram of the experimental system is shown in Fig. 1. The test section (Fig. 2) was a rectan-

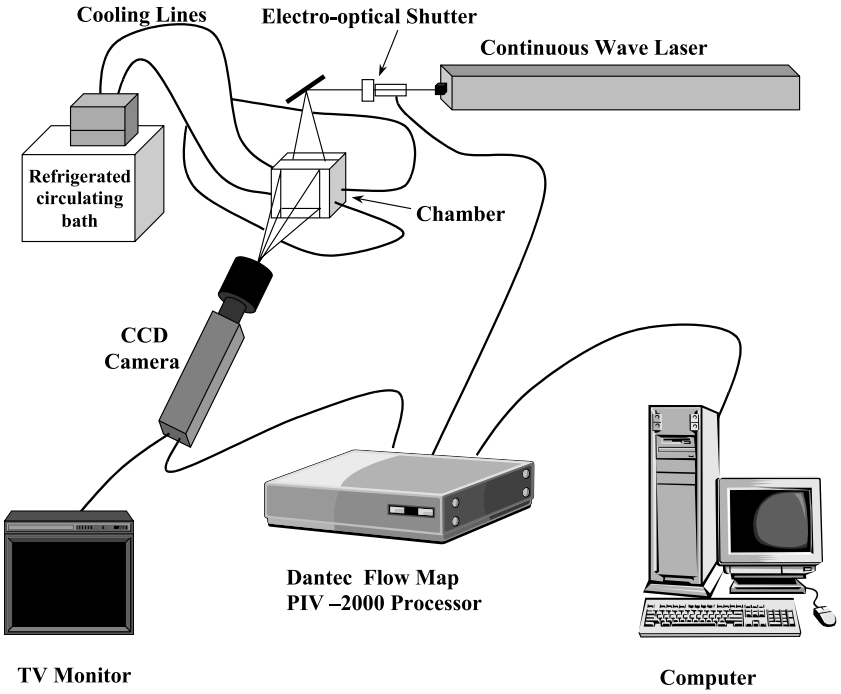

Fig. 1. Schematic diagram of the PIV measurement system.

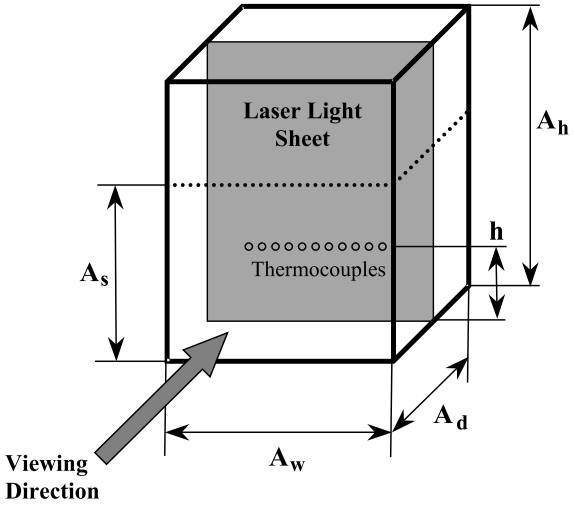

Fig. 2. Schematic diagram of the test chamber.

gular chamber with inside dimensions of 81 mm wide (A_w), 125 mm high (A_h), and 104 mm deep (A_d). The aspect ratio was 1.28 (A_d/A_w), which was sufficiently large to render three-dimensional effects negligible [17]. The chamber was cooled along two of the vertical sidewalls. The cooling walls were made of copper plates with channels for circulating coolant liquid. The other walls were made of 13 mm-thick Plexiglass. The rectangular chamber was chilled with NESLAB Endocal Refrigerated Circulating Bath using ethylene glycol as the cooling medium. The temperature distribution in the solution was obtained by means of 11 type E thermocouples mounted on a horizontal rake. The rake was installed 20 mm away from the rear plate of the test chamber. The width of the thermocouple rake was 50 mm, compared to the width of the test chamber at 81 mm; therefore, the local temperature data near the chamber walls were not obtained from the current experiment. The rake was positioned at a vertical location within the test chamber, corresponding to an elevation of $h = 32$ mm from the bottom of the chamber as shown in Fig. 2. The position of the sixth thermocouple was aligned to the central axis of the test chamber, and the spacing between adjacent thermocouples was 5 mm. The output voltages of the thermocouples were measured using a National Instruments data acquisition system.

2.2. PIV system

The PIV system from DANTEC was used to obtain the velocity flow fields with high accuracy and high resolution. In this system, the laser beam from CW argon-ion laser passed through light-sheet-creating optics and formed a thin light sheet to illuminate the seeding particles in the solution. The beam from the CW laser was chopped into pulses with a known time separation by DANTEC's 80X41 electro-optical shutter. The time

separation between the pulses was selected depending on the vigor of the convective flow during the solidification. DANTEC's 80C42 DoubleImage 700 camera was used to record images of an illuminated section. The DoubleImage 700 camera contains a video format CCD chip and special electronics for fast interframe acquisition of two images. The image size was 768×484 pixels. The images were preprocessed with the DANTEC's PIV2000 processor. Post-processing and data analysis of the images were performed on a PC. A Sony TV monitor was connected to the CCD camera and used to visualize the process of solidification online.

Proper selection of the seeding particles is crucial to the quality of the measurement by the PIV technique. In this respect, the particles must be small enough to track the flow accurately but large enough to form a proper size image to be visible. In addition, the seeding particles should be neutrally buoyant in the liquid under investigation. Practically, the settling velocities have to be much smaller than the fluid velocity of the flow under investigation. In this study, Polyamide seeding particles were used that had a mean particle diameter of 20 μm and density of 1030 kg/m^3. The calculated settling velocity was 2.3×10^{-6} m/s, which is several orders of magnitude lower than the average flow velocity determined from experimental measurements. Thus, these seeding particles were considered suitable.

2.3. Binary solution

Aqueous ammonium chloride (NH_4Cl–H_2O) solution was selected as the test fluid because the behavior of this aqueous salt solution is analogous to metallic alloy melts and has the advantage of being transparent so that the convection pattern and the dynamics of the solid–liquid interface may be visualized. Many researchers [2,7,8,18,19] have used NH_4Cl–H_2O as an analogue system to study the solidification process in metallic alloys. The thermo-physical properties of the aqueous ammonium chloride solution are well documented. The equilibrium phase diagram for aqueous ammonium chloride is shown in Fig. 3. The diagram shows that the eutectic concentration of the solution C_e is 19.7 wt.% and the eutectic temperature T_e is −15.4 °C.

3. Experimental procedure

To begin the experiment, a solution of the desired concentration was prepared by mixing corresponding amounts of ammonium chloride and distilled water. When all of the ammonium chloride was dissolved, the initial homogeneous solution was achieved, and the solution was poured into the chamber. The total volume (500 ml) and initial temperature (20 °C) of the solution were kept the same for all test runs. The height-to-width

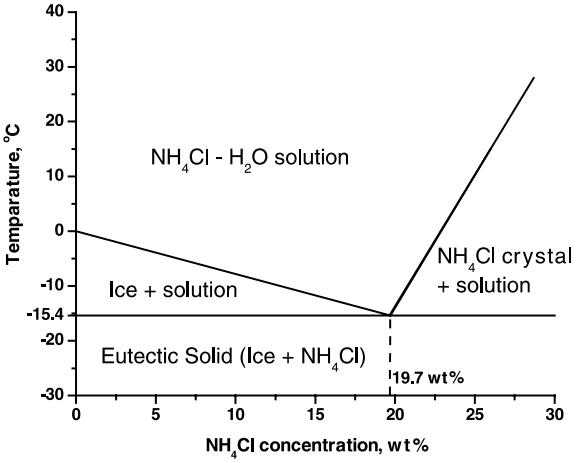

Fig. 3. Equilibrium phase diagram for NH_4Cl–H_2O solution.

ratio of the chamber occupied by the solution was ≈0.88. While the solution was prepared, the circulating bath was brought to the required cooling temperature. The circulation of the coolant along the two sidewalls of the test chamber was started to begin the solidification process. The temperature of the output coolant in the chiller was set at −20 °C for all test runs. Once the experiment started, the data acquisition system was activated to record the temperature readings continuously. DANTEC's Flow Manager software was used to capture image maps and to determine the velocity flow fields during the solidification process. The image maps and the velocity fields were recorded every seven minutes from the start of the solidification experiment. When there were no significant variations in the velocity flow fields with respect to time, the data acquisition of the solidification experiment was stopped.

4. Uncertainty analysis

The complexity of the measurements gives rise to numerous sources of uncertainty, of which only the most important are discussed here. The positioning uncertainty of the measurement plane formed by the laser sheet was minimized in the present study. The alignment of the laser sheet was carefully conducted to insure that the laser sheet was parallel to the front window of the chamber. The error was estimated at 0.5%. The standard limit of the uncertainty of a type E thermocouple is 1.7 °C. The preparation of binary solution gives rise to an uncertainty of the obtained concentration of less than 1%. Thus, the measurement uncertainty incurred from the uncertainty of concentration of solution was negligible. The uncertainty of the PIV operation mode on the determination of the flow field has been discussed elsewhere; the double-frame cross-correlation mode was

adopted here [20]. The interrogation sub-domain of 16 by 16 pixels without overlap was used in the present PIV measurement.

5. Experimental results and discussions

5.1. Convection patterns

Convection patterns for various initial concentrations of aqueous ammonium chloride solution were studied during the solidification process. The concentration of the solution ranged from 10 to 22 wt.%. The initial solute concentration of the binary solution was assumed to be homogeneous. The evolutions of the convection patterns for different ammonium chloride concentrations are shown in Figs. 4, 5 and 7. The dark thick vertical line in the figures represents the cooling walls along the two sides of the chamber; the dashed line at the bottom is the adiabatic insulated wall. The thin solid vertical line represents the solidified layer formed on the sidewall, which had almost uniform thickness along both cooling walls. The locations of the thermocouple tips relative to the flow field are represented by an array of circles depicted in the first vector plot of the series in each figure.

A set of the convection patterns for the solidification process of 10 wt.% NH_4Cl–H_2O solution is shown in Fig. 4. Fig. 4a and b show the initial stages of the process at 7 and 14 min from the start of the solidification

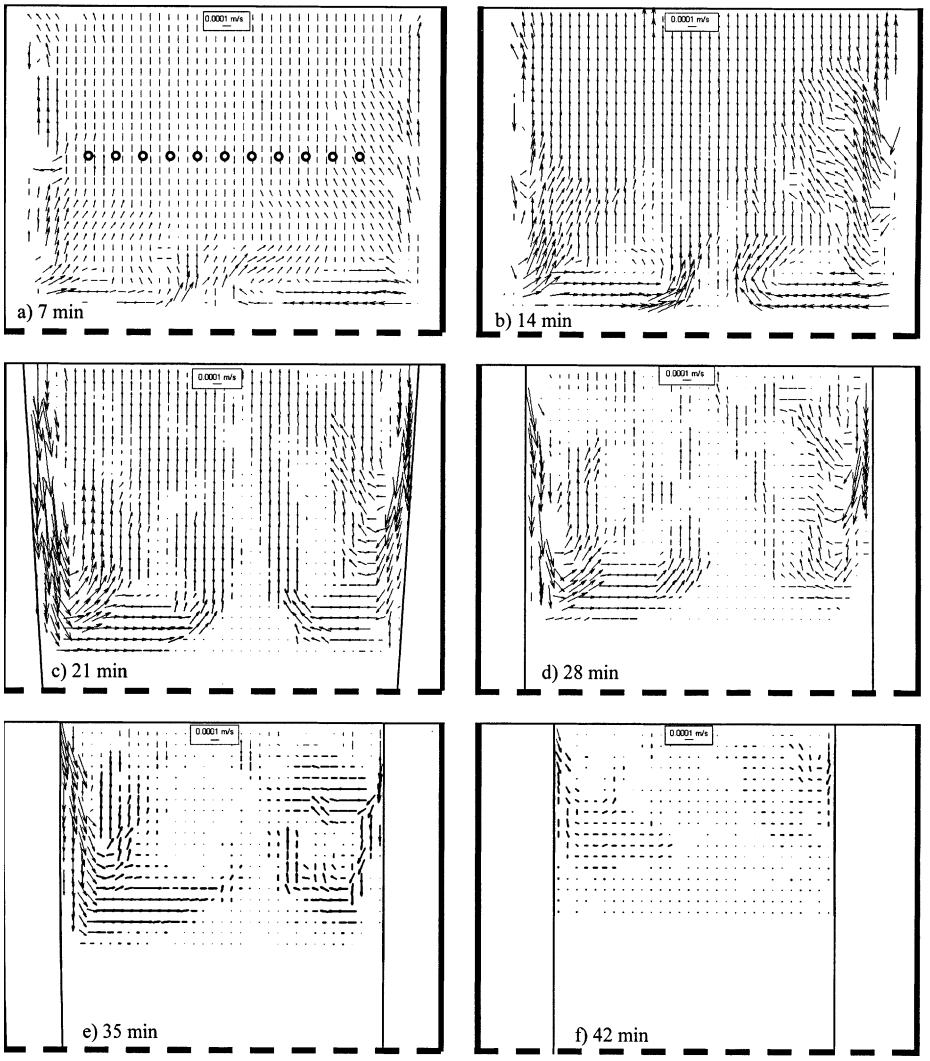

Fig. 4. The evolution of the convection patterns for 10 wt.% aqueous ammonium chloride solution. (The position of the thermocouple rake for temperature measurements is shown in the plot (a) as an array of circles.)

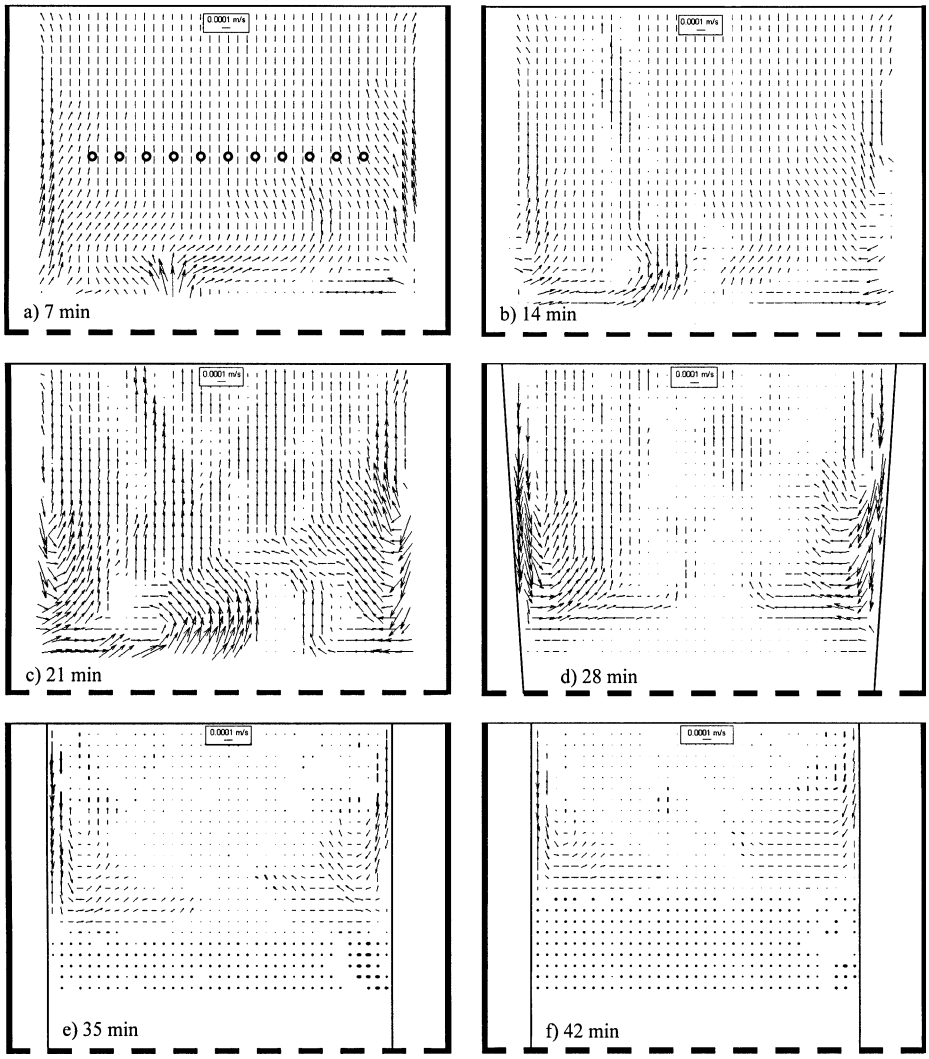

Fig. 5. The evolution of the convection patterns for 15 wt.% aqueous ammonium chloride solution. (The position of the thermocouple rake for temperature measurements is shown in the plot (a) as an array of circles.)

process. Formation of two major counter-rotating convective cells is seen on these figures: The flow in the left cell is counterclockwise, and that in the right cell is clockwise. These convective cells are formed by the vertical downward flow of heavier solute-rich liquid produced upon solidification along the cooling walls of the chamber followed by horizontal flow at the bottom of the chamber from the cooling walls to the center and upward flow throughout most of the chamber interior. The downward flow in the thin layer along the cooling walls was not seen at this initial stage of the process because the front window gasket was blocking the view of about 4 mm along the walls. However, this flow is clearly seen at the later stages of the process (Fig. 4c–f), when the solidified layer grew beyond the front window gasket. The flow velocity of the downward flow along the cooling walls is always higher than that of upward flow in the bulk of the chamber as indicated by the length of velocity vectors. The magnitude of the velocity vectors also shows that the convection is more vigorous at the beginning of the solidification process and gradually slows down as the process progresses. Fig. 4c–f shows that with the progress of solidification, the solidified layers on both cooling walls are growing. Heavy solute-rich liquid continues to accumulate at the bottom of the chamber and remains stagnant. The counter-rotating convective cells are moving upward, being pushed by heavy solute-rich liquid accumulating at the bottom.

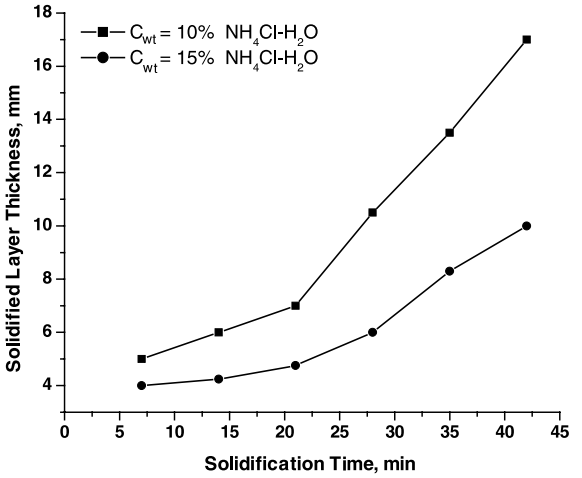

Fig. 6. Solidified layer thickness versus time for concentrations of 10 and 15 wt.% aqueous ammonium chloride solutions.

A set of the convection patterns for the solidification process of 15 wt.% NH_4Cl–H_2O solution is shown in Fig. 5. The convection patterns during the solidification process of 15 wt.% solution are fundamentally similar to those of 10 wt.%. Fig. 5 shows that as with 10 wt.%, two counter-rotating convective cells are present due to the downward flow of heavier solute-rich liquid produced upon solidification along the cooling walls. The downward flow along the walls is more intense than the upward flow throughout the remainder of the chamber. As in the case of 10 wt.%, the convective flow in 15 wt.% solution decelerates with the progress of solidification. Growth of solidified layers on cooling walls and accumulation of heavy solute-rich liquid at the bottom of the chamber are slower at 15 wt.% than at 10 wt.% due to lower liquidus temperature for the former.

The solidified layer thickness versus time for solidification of hypoeutectic concentrations of NH_4Cl–H_2O solution is shown in Fig. 6. The thickness is obtained by measuring the thickness of the layer on an image at the half-height from the bottom. The figure shows that the solidified layer thickness for both concentrations increases linearly after $t = 21$ min from the start of the solidification experiment. Solidified layer grows faster for 10 wt.% concentration as indicated by the slope of the curve. It is also noted from the visualization that the solidified layer grows almost uniformly over both vertical walls.

The evolution of the convection patterns for the solidification process of 22 wt.% NH_4Cl–H_2O solution is shown in Fig. 7. The initial stage of the solidification process is not shown in Fig. 7 since the flow visualization shows that the flow pattern was unsteady. For this hypereutectic concentration, lighter water-rich liquid is released during solidification. This lighter liquid accumulates at the top of the chamber and creates a thermally unstable but solutally stable condition, resulting in formation of vertically stacked layers of double-diffusive convective cells (Fig. 7a) separated by density fronts [10]. There are three layers of convective cells in Fig. 7a, with clockwise rotating cells on the right-hand side and counterclockwise cells on the left-hand side in each layer. With the progress of solidification (Fig. 7b–f), lighter water-rich liquid continues to accumulate at the top of the chamber. This creates new layers of double-diffusive convective cells (Fig. 7c), while older layers are pushed downward. At this concentration, large numbers of dendrites grow and break off the cooling walls with subsequent accumulation in the bottom corners of the chamber. Heaps of dendrites obstructed the view and made it impossible for the PIV system to detect the flow in the corner areas, as discussed previously [14]. As the solidification process goes on, double-diffusive cells move slowly downward. Flow velocities in the cells increase after cell formation, remain approximately constant as cells evolve and move downward, and decrease as cells collapse at the bottom of the chamber.

From the experimental observations of 10 and 15 wt.% concentrations (hypoeutectic growth) and 22 wt.% concentration (hypereutectic growth), it is evident that the initial solutal concentration determines the number and evolution of the convective cells during the solidification process. For the solidification of 10 and 15 wt.% concentration solutions, the number of formed convective cells is constant throughout the process and is equal to two, and these cells move upward with the progress of the solidification. Whereas for the solidification of 22 wt.% concentration solution, the number of convective cells is changing as new double-diffusive layers appear at the top of the chamber, while the old ones disappear at the bottom. The vigor of convective flow gradually decreases with the progress of solidification for 10 and 15 wt.%, while for 22 wt.%, it remains approximately steady.

5.2. Temperature distribution

The temperature distribution in the horizontal direction 32 mm above the chamber bottom was measured with the rake of 11 thermocouples. Measurements taken at the same time as flow field acquisitions for all tested binary solution concentrations are presented in Figs. 8–10. For the cases of 10 and 15 wt.%, the temperature profiles are very similar and almost constant along the rake. These profiles are not affected by the convective flow and remain uniform with the progress of the

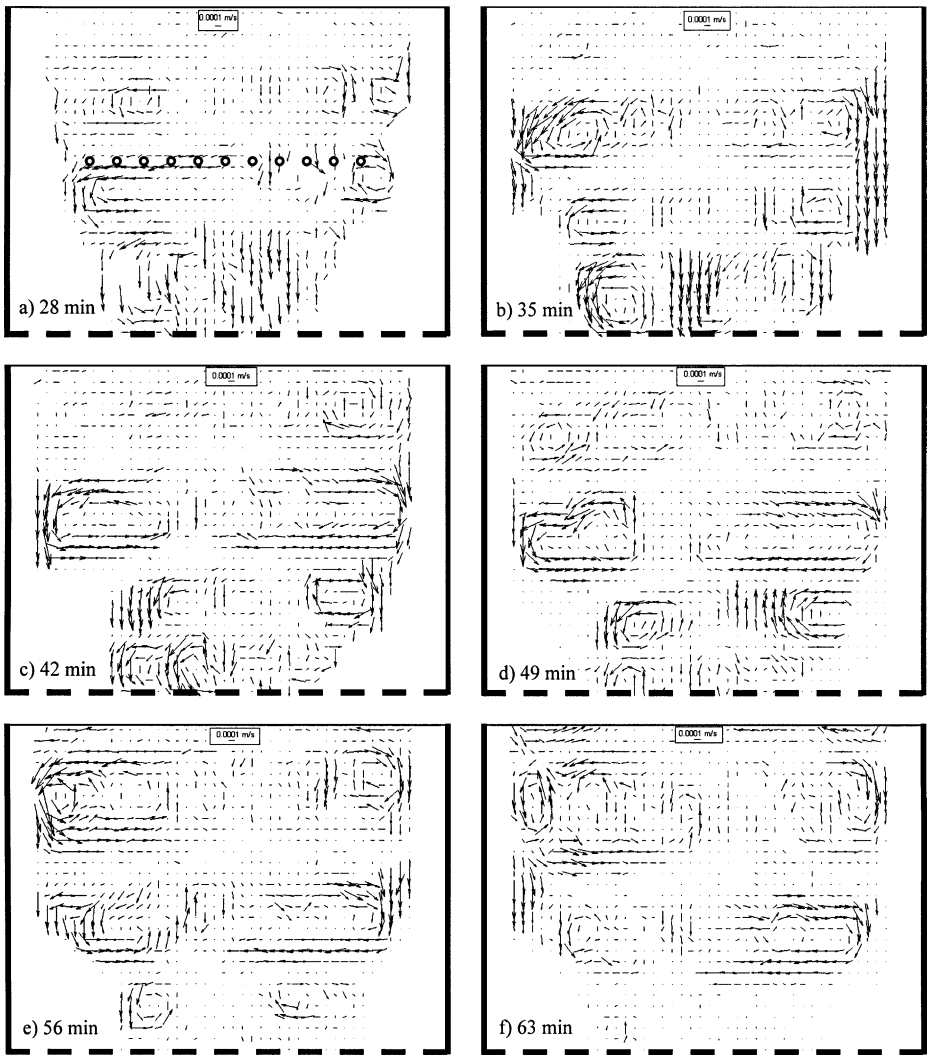

Fig. 7. The evolution of the convection patterns for 22 wt.% aqueous ammonium chloride solution. (The position of the thermocouple rake for temperature measurement is shown in the plot (a) as an array of circles.)

solidification, with average temperature gradually decreasing. For the case of 22 wt.% (Fig. 10), the temperature profiles have parabolic shape with the maximum close to the chamber central axis. As the solidification progresses, the temperatures decrease from $t = 28$ to 42 min; however, the temperatures increase thereafter, up to $t = 63$ min. This temperature behavior is associated with the layer of convective cells passing by the thermocouple rake. As seen in Fig. 7, from $t = 28$ to 35 min, a stagnant interlayer region is passing by the thermocouple rake. At $t = 42$ and 49 min, the thermocouple rake is inside the layer of convective cells, which is reflected by very close temperature profiles at these times in Fig. 10. Thereafter, another interlayer region starts to pass by the thermocouple rake, which results in increasing temperatures. Such phenomena were also observed by Nushimura et al. [9] in a rectangular chamber with one cooled sidewall.

6. Conclusions

The purpose of the present study was to characterize the influence of the initial concentration during the solidification of aqueous ammonium chloride solution on the evolution of the convection patterns. A PIV system was used to visualize the convection. The advantage of the PIV technique is its ability to obtain accurate quantitative data without disturbing the flow field. Convection patterns and temperature distributions in certain locations were measured for the initial concentrations of ammonium chloride solution ranging from

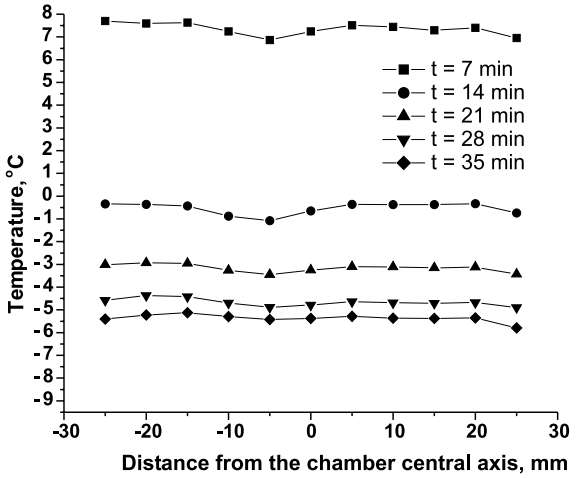

Fig. 8. Temperature distribution in the horizontal direction for 10 wt.% aqueous ammonium chloride solution.

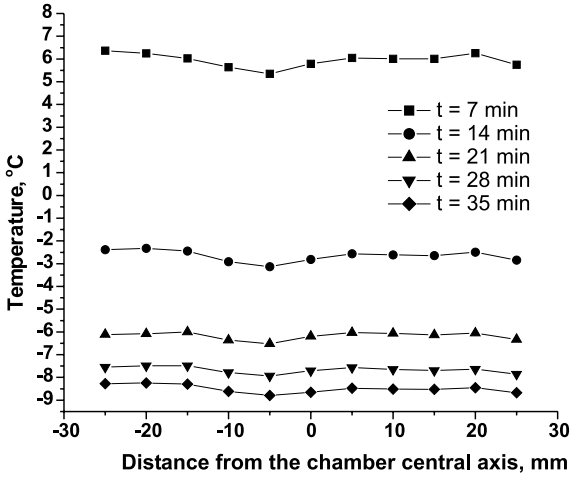

Fig. 9. Temperature distribution in the horizontal direction for 15 wt.% aqueous ammonium chloride solution.

10 to 22 wt.%. The evolution of the convective flow driven by double-diffusive force was found to be a time-transient phenomenon. The convection pattern was characterized by a pair of convective cells for the hypo-eutectic concentration of NH_4Cl, such as 10 wt.%. For the hypereutectic concentration of NH_4Cl solution such as 22 wt.%, the convection pattern was characterized by vertically stacked layers of double-diffusive convective cells.

In addition, the quantitative data for convection patterns obtained from the PIV measurement and the information on the solidified layer thickness could provide a benchmark data set for the validation of the numerical predictions based on the CFD simulation and for the model development of phase-changing processes.

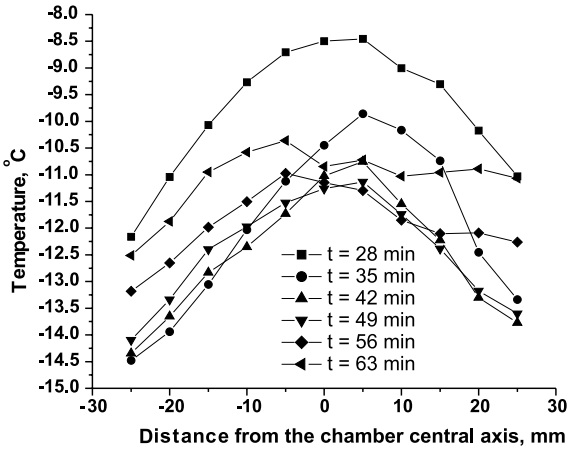

Fig. 10. Temperature distribution in the horizontal direction for 22 wt.% aqueous ammonium chloride solution.

Acknowledgements

The research was made possible by grants sponsored by the US National Science Foundation and by the US Department of Energy.

References

[1] M.G. Worster, Convection in mushy layers, Ann. Rev. Fluid Mech. 29 (1997) 91–122.
[2] G. Hansen, A. Hellawell, S.Z. Lu, R.S. Steube, Some consequences of thermosolutal convection: the grain structure of castings, Metall. Mater. Trans. A: Phys. Metall. Mater. Sci. 27A (3) (1996) 569–581.
[3] S.L. Braga, R. Viskanta, Solidification of a binary solution on a cold isothermal surface, Int. J. Heat Mass Transfer 33 (1990) 745–754.
[4] C. Beckermann, R. Viskanta, Double-diffusive convection during dendritic solidification of a binary mixture, Phys. Chem. Hydrodyn. 10 (1988) 195–213.
[5] C. Beckermann, R. Viskanta, Forced convection boundary layer flow and heat transfer along a flat plate embedded in a porous medium, Int. J. Heat Mass Transfer 30 (1987) 1547–1551.
[6] C. Beckermann, S. Ramadhyani, R. Viskanta, Natural convection flow and heat transfer between a fluid layer and a porous layer inside a rectangular chamber, J. Heat Transfer, Trans. ASME 109 (1987) 363–370.
[7] M.S. Christenson, F.P. Incropera, Solidification of an aqueous ammonium chloride solution in a rectangular chamber- I. Experimental study, Int. J. Heat Mass Transfer 32 (1989) 47–68.

[8] M.S. Christenson, W.D. Bennon, F.P. Incropera, Solidification of an aqueous ammonium chloride solution in a rectangular chamber-II. Comparison of predicted and measured results, Int. J. Heat Mass Transfer 32 (1989) 69–79.

[9] T. Nishimura, M. Fujiwara, N. Horie, H. Miyashita, Temperature visualizations by use of liquid crystals of unsteady natural convection during super cooling and freezing of water in a chamber with lateral cooling, Int. J. Heat Mass Transfer 34 (1991) 2663–2668.

[10] T. Nishimura, T. Imoto, H. Miyashita, Occurrence and development of double-diffusive convection during solidification of a binary system, Int. J. Heat Mass Transfer 37 (10) (1994) 1455–1464.

[11] H. Han, T.H. Kuehn, Double-diffusive natural convection in a vertical rectangular chamber-II. Numerical study, Int. J. Heat Mass Transfer 34 (1991) 461–471.

[12] Z.F. Dong, M.A. Ebadian, Investigation of double-diffusive convection in a trapezoidal enclosure, J. Heat Transfer, Trans. ASME 116 (1994) 492–495.

[13] Z.F. Dong, M.A. Ebadian, Numerical simulation of double-diffusive convection in a V-shaped sump, Int. J. Heat Mass Transfer 16 (1995) 236–243.

[14] S.Y. Wang, C.X. Lin, M.A. Ebadian, Study of double-diffusive velocity during the solidification process using particle image velocimetry, Int. J. Heat Mass Transfer 42 (1999) 4427–4445.

[15] S.Y. Wang, C.X. Lin, M.A. Ebadian, Vortex flow of low concentration NH_4Cl–H_2O solution during the solidification process, Int. J. Heat Mass Transfer 42 (1999) 4153–4163.

[16] N. Pradeep, H.J. Kang, C.X. Lin, M.A. Ebadian, The influence of boundary condition on solidification of binary solution in rectangular cavity, Proc. ASME, Heat Transfer Div. 2 (2000) 185–190.

[17] B. Gebhart, Y. Jaluria, R.L. Mahajan, B. Sammakia, Buoyancy-induced flows and transport, Hemisphere Publishing Co, New York, 1988, Chapter 14.5.

[18] K.A. Jackson, J.D. Hunt, D.R. Uhlmann, T.P. Seward, On the origin of the equiaxed zone in castings, Trans. Metall. Soc. AIME 236 (1966) 149–158.

[19] C.F. Chen, Experimental study of convection in a mushy layer during directional solidification, J. Fluid Mech. 293 (1995) 81–98.

[20] Dantec Measurement Technology, FlowMap—Installation & User's Guide, Publication No. 9040U3622, Skovulunde, Denmark, 1997.